Journal of Solid Mechanics Vol. 4, No. 1 (2012) pp. 15-32

Electro-Thermo-Dynamic Buckling of Embedded DWBNNT Conveying Viscous Fluid

A. Ghorbanpour Arani [1,2*], M. Hashemian[2]

[1]*Faculty of Mechanical Engineering, University of Kashan, Kashan, Islamic Republic of Iran*
[2]*Institute of Nanoscience & Nanotechnology, University of Kashan, Kashan, Islamic Republic of Iran*

Received 7 November 2011; accepted 4 January 2012

ABSTRACT

In this paper, the nonlinear dynamic buckling of double-walled boron-nitride nanotube (DWBNNT) conveying viscous fluid is investigated based on Eringen's theory. BNNT is modeled as an Euler-Bernoulli beam and is subjected to combine mechanical, electrical and thermal loading. The effect of viscosity on fluid-BNNT interaction is considered based on Navier-Stokes relation. The van der Waals (vdW) interaction between the inner and outer nanotubes is taken into account and the surrounding elastic medium is simulated as Winkler and Pasternak foundation. Considering the charge equation for coupling of mechanical and electrical fields, Hamilton's principle is utilized to derive the motion equations based on the von Kármán theory. Dynamic buckling load is evaluated using differential quadrature method (DQM). Results show that dynamic buckling load depends on small scale factor, viscosity, elastic medium parameters and temperature changes. Also, dynamic instability region is discussed for various conditions. © 2012 IAU, Arak Branch. All rights reserved.

Keywords : Dynamic Buckling ;DWBNNT ; Viscous Flow ;Pasternak Medium ;DQM

Archive of SID

1 INTRODUCTION

WITH discovery of BNNTs in 1995, increasing researches have been conducted on these materials. BNNTs have excellent chemical and thermal stability, so they can be used in equipments with high thermal resistance. BNNTs are in amorphous and crystalline forms and unlike carbon nanotubes (CNTs), have strong piezoelectric property. This property makes them a novel choice for producing sensors and actuators. The electrical properties of CNTs are very variable and change between metallic and semiconducting materials, but BNNTs have been considered as semiconductors, so they have stable electrical properties also.

Recently nanotubes are used as vessels for keeping fluid and solid particles; also they can transfer vitamins and proteins in medicine equipments. It should be noticed that flowing fluid induces electric potential due to piezoelectric property. Flow-induced instability of nanotubes is one of the popular topics these years and many papers have been studied the vibration and stability of CNTs. In continuum mechanics, nano structures have been considered as continuous beams, so investigating the behaviors of beams are very essential in nanotubes studies [1],[2].

Vibration and stability of tubes containing fluid have been studied in literature. Païdousis [3], in 1998, examined the effect of flowing fluid in pipes and other structures and several articles are based on the results of this work. Amabili et al. [4] studied nonlinear dynamics of cylindrical shells conveying flowing fluid and used Auto software. They also obtained divergence velocity for imperfective circular cylindrical shell [5]. The effect of viscosity on nonlinear dynamics of cylindrical shells is reported by Karagiozis et al. [6]. Païdoussis et al. [7] investigated coaxial

* Corresponding author. Tel.: +98 9131626594 ; Fax: +98 361 55912424
E-mail address: aghorban@kashanu.ac.ir (A.Ghorbanpour Arani).

© 2012 IAU, Arak Branch. All rights reserved.

www.SID.ir

cylindrical shells conveying viscous fluid, results show that viscosity destabilize the shell. Ni et al. [8] implied differential transformation method (DTM) for pipes conveying fluid.

The properties of CNTs as fluid transmitter can be observed recently. Yan [9] reported the stability of triple-walled carbon nanotubes conveying fluid; nanotube is modeled as an Euler-Bernoulli beam and the frequency of beam is derived. Also, the role of internal flow and vdw forces on the stability of CNTs is investigated in this analysis. Yoon et al. [10] studied the influence of internal flowing fluid on resonant frequency. Wang [11] utilized the nonlocal elasticity theory [12] in study of vibration and instability of nano beams conveying fluid and small length specified as an effective parameter on critical flow velocity. Ke et al. [13] considered small scale effect according to couple stress theory and studied the vibration and stability of DWCNTs, differential quadrature method (DQM) is used in this survey. The effect of viscoelastic Winkler foundation on the instability of CNTs conveying fluid is studied by Ghavanloo et al. [14]. Considering the viscous fluid in CNTs is reported by Khosravian et al. [15] for the first time and improved by Wang et al. [16], results show that the effect of viscosity on the instability of CNTs can be neglected.

As mentioned in the first paragraph, BNNTs have piezoelectric properties that can be used in smart control. Few studies have been done on the properties of BNNTs. Salehi-khojin and jalili [17] investigated the buckling of BNNT reinforced piezoelectric polymeric composites under different loadings. Results show that buckling resistance of polymeric composite increases by BNNT reinforcement. Ghorbanpour Arani et al. [18] studied the axial buckling of DWBNNTs considering the nonlocal piezoelasticity. In above articles the coupling between electrical and mechanical fields is neglected. Recently, torsional buckling of a piezoelectric polymeric cylindrical shell reinforced by DWBNNTs is investigated by Mosallaie et al. [19] considering the coupling between electrical and mechanical fields.

In mentioned articles static linear buckling load is evaluated. Unlike above studies in this work the charge relation is taken into account and electro-thermo nonlinear nonlocal dynamic buckling of clamped supported DWBNNT conveying viscous fluid is investigated. Using Hamilton's principle, the couple governing equations are derived and DQM is presented to estimate the dynamic buckling load of DWBNNTs. Small scale effects, vdW forces, Pasternak foundation and viscous fluid are considered in this survey.

2 DERIVING MOTION EQUATIONS

A DWBNNT conveying flowing fluid is shown in Fig. 1. The cylindrical coordinate is used in this study and the displacement components in the x, θ and z directions are shown by u, v and w respectively. R_1 and R_2 are the internal radiuses of inner and outer tubes, L is the length, h is the thickness of tubes, V_∞ is the flow velocity and DWBNNT is embedded in an Pasternak medium under electrical loading.

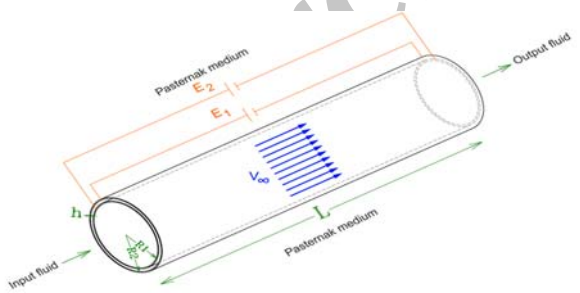

Fig.1
DWBNNT conveying fluid embedded in Pasternak medium.

2.1 Fluid-BNNT interaction

The velocity components of the flowing fluid in the axial and radial directions can be expressed as [3]:

$$V_x = \frac{\partial u_1}{\partial t} + V_\infty \cos(\alpha), \tag{1}$$

© 2012 IAU, Arak Branch

www.SID.ir

$$V_r = \frac{\partial w_1}{\partial t} + V_\infty \sin(\alpha), \tag{2}$$

where α represents the attack angle of flow and u_1 and w_1 are the middle surface displacements of the inner tube. Above equations can be simplified by considering $\cos(\alpha) = 1$ and $\sin(\alpha) = \frac{\partial w}{\partial x}$, [3] as:

$$V_x = \frac{\partial u_1}{\partial t} + V_\infty, \tag{3}$$

$$V_r = \frac{\partial w_1}{\partial t} + V_\infty \frac{\partial w_1}{\partial x}. \tag{4}$$

To evaluate the interaction between DWBNNT and fluid, Navier-Stokes equation can be used as [16]:

$$\rho_f \frac{DV}{Dt} = -\nabla p + \rho_f g + \mu \nabla^2 V, \tag{5}$$

where μ, ρ_f and p are the viscosity, density and pressure of the fluid respectively and $\frac{D}{Dt}$ represents the material derivative. Eq. (5) can be expanded in the r direction considering Eqs. (3) and (4) as:

$$\frac{\partial p}{\partial r} = -\rho_f \left(\frac{\partial^2 w_1}{\partial t^2} + 2V_\infty \frac{\partial^2 w_1}{\partial x \partial t} + \frac{\partial u_1}{\partial t} \frac{\partial^2 w_1}{\partial x \partial t} + \frac{\partial u_1}{\partial t} V_\infty \frac{\partial^2 w_1}{\partial x^2} + V_\infty^2 \frac{\partial^2 w_1}{\partial x^2} \right) + \mu \frac{\partial^3 w}{\partial x^2 \partial t} + \mu V_\infty \frac{\partial^3 w}{\partial x^3}. \tag{6}$$

The above equation indicates force per unit volume in the r direction, so it can be used to evaluate fluid-BNNT interaction. The energy of the fluid-DWBNNT interaction can be obtained as [4]:

$$W_f = \int_A \int_0^L \frac{\partial p}{\partial r} w_1 \, dx \, dA \tag{7}$$

2.2 Strain- displacement relation

In this study von Kármán nonlinear equation is used to state the relation between strain and displacement components. Displacement field is considered as [26]:

$$\begin{aligned} \bar{u}_i(x,z,t) &= u_i(x,z,t) - z \frac{\partial w_i(x,z,t)}{\partial x} \\ \bar{w}_i(x,z,t) &= w_i(x,z,t) \qquad i = 1,2 \end{aligned} \tag{8}$$

where $\bar{u}_i$ and $\bar{w}_i$ represent the total displacement of the i^{th} tube and u_i and w_i are the middle surface displacements. Using Eq. (8), the strain-displacement relation based on the von Kármán nonlinear theory can be expressed as [26]:

$$\varepsilon_{xi} = \frac{\partial u_i}{\partial x} + \frac{1}{2}\left(\frac{\partial w_i}{\partial x} \right)^2 - z\left(\frac{\partial^2 w_i}{\partial x^2} \right) \tag{9}$$

© 2012IAU, Arak Branch

Archive of SID

www.SID.ir

2.3 Strain energy of the beams

The governing equations in this study are derived using energy method. The strain energy for Euler-Bernoulli beam is:

$$\Pi_i = \int_{A_i}\int_0^L \sigma_{xi}\varepsilon_{xi}\, dx\, dA, \tag{10}$$

where σ_{xi} and ε_{xi} represent the axial stress and strain components of the i^{th} BNNT and A_i represents the cross section area of the i^{th} tube. The variation form of the strain energies for the inner and outer tubes are obtained after substituting Eq. (9) into Eq. (10) as:

$$\delta\Pi_i = \delta\left(\int_{A_i}\int_0^L \sigma_{xi}\varepsilon_{xi}\, dx\, dA\right) = -\int_0^L \frac{\partial N_{xi}}{\partial x}\delta u_i\, dx - \int_0^L \left(\frac{\partial}{\partial x}\left(N_{xi}\frac{\partial w_i}{\partial x}\right) + \frac{\partial^2 M_{xi}}{\partial x^2}\right)\delta w_i dx, \tag{11}$$

where $N_{xi} = \int \sigma_{xi}\, dA$ and $M_{xi} = \int \sigma_{xi}\, z\, dA$ are the force and momentum implied on the i^{th} tube.

2.4 Kinetic energy of the beams

The kinetic energy of the beam and the variation form can be expressed as:

$$T_i = \frac{\rho_t}{2}\int_{A_i}\int_0^L \left[\left(\frac{\partial u_i}{\partial t} - z\frac{\partial^2 w_i}{\partial x\,\partial t}\right)^2 + \left(\frac{\partial w_i}{\partial t}\right)^2\right] dx\, dA_i, \tag{12}$$

$$\int_0^t \delta T_i\, dt = -\rho_t \int_0^t\int_0^L \frac{\partial^2 u_i}{\partial t^2}A_i\delta u_i\, dx\, dt + \rho_t\int_0^t\int_0^L\left(I_i\frac{\partial^4 w_1}{\partial x^2\partial t^2} - A_i\frac{\partial^2 w_1}{\partial t^2}\right)\delta w_i\, dx\, dt. \tag{13}$$

where ρ_t is the density of BNNTs in above equations.

2.5 Kinetic energy of the fluid

The kinetic energy of the fluid and its variation form can be obtained using Eqs. (3) and (4), as:

$$T_f = \int_{A_f}\int_0^L \frac{\rho_f}{2}\left[\left(\frac{\partial u_1}{\partial t} + V_\infty\right)^2 + \left(\frac{\partial w_1}{\partial t} + V_\infty\frac{\partial w_1}{\partial x}\right)^2 + z^2\left(\frac{\partial^2 w_1}{\partial x\,\partial t}\right)^2\right] dx\, dA, \tag{14}$$

$$\begin{aligned}\int_0^t \delta T_f = -\rho_f\int_0^t\int_0^L\Bigg[&A_f\frac{\partial^2 u_1}{\partial t^2}\delta u_1 + \left(A_f\frac{\partial^2 w_1}{\partial t^2} + A_f V_\infty\frac{\partial^2 w_1}{\partial x\,\partial t}\right)\delta w_1 \\ &+ A_f V_\infty\frac{\partial^2 w_1}{\partial x\,\partial t} + A_f V_\infty^2\frac{\partial^2 w_1}{\partial x^2} - I_f\frac{\partial^4 w_1}{\partial x^2\partial t^2}\Bigg] dx\, dt\end{aligned} \tag{15}$$

where $A_f = \dfrac{\pi R_1^2}{4}$, represents the area that fluid passes through the inner BNNT.

© 2012 IAU, Arak Branch

www.SID.ir

2.6 Electric field energy

This energy is expressed as below according to [20] :

$$W_e = \int_V D_{xi} E_{xi} dV, \tag{16}$$

where D_x and E_x are the electric displacement and electric field in the axial direction for the i^{th} tube respectively. Relation between electric field and electric potential is expressed as:

$$E_{xi} = -\frac{\partial \varphi_{xi}}{\partial x}, \tag{17}$$

So variation form of Eq. (16) can be derived as:

$$\delta W_e = -\int_V \frac{\partial D_{xi}}{\partial x} \delta \varphi_{xi} dV. \tag{18}$$

2.7 Surrounding medium energy

The elastic medium in this study is considered as Winkler and Pasternak foundation. The interaction between this medium and outer surface of the 2nd BNNT according to [21] is:

$$F_m = K_w w_2 - K_g \frac{\partial^2 w_2}{\partial x^2}, \tag{19}$$

where K_w is the spring constant of the Winkler foundation and K_g is the shear constant of the Pasternak foundation. The variation form of the medium energy can be stated as [22]:

$$\delta W_m = -\int_0^L 2\pi R_{o2} \left(K_w w_2 - K_G \frac{\partial^2 w_2}{\partial x^2} \right) \delta w_2 dx \tag{20}$$

where R_{o2} represents the outer radious of the 2nd BNNT.

2.8 Energy of the Van der Waals interaction

The pressure exerted on the 1st and 2nd nanotubes due to the vdW interaction can be expressed as [23, 24]:

$$F_1^v = c(w_2 - w_1), \tag{21a}$$

$$F_2^v = -\frac{R_{1o}}{R_2} c(w_2 - w_1), \tag{21b}$$

where c is the vdW coefficient and R_{o1} is the outer radius of the inner BNNT, so the variation of this energy can be written as [25]:

$$\delta W_v = \int_0^L 2\pi R_{o1} c(w_2 - w_1) \delta w_1 dx - \int_0^L 2\pi R_{1o} c(w_2 - w_1) \delta w_2 dx \tag{22}$$

© 2012IAU, Arak Branch

Archive of SID

www.SID.ir

2.9 Hamilton's principle

The motion equations of embedded DWBNNT conveying viscose fluid can be derived by Hamilton's principles as follows:

$$\int_0^t \left(\delta\Pi_1 + \delta\Pi_2 - \delta T_1 - \delta T_2 - \delta T_f - \delta W_m - \delta W_v - \delta W_e - \delta W_f\right) = 0. \tag{23}$$

Integrating Eq. (23) by parts and setting the coefficient of mechanical (δu_i, δw_i) and electrical ($\delta\varphi_i$) displacements to zero, lead to the following motion equations:

$$-\frac{\partial N_{x1}}{\partial x} + \rho_t A_1 \frac{\partial^2 u_1}{\partial t^2} + \rho_f A_f \frac{\partial^2 u_1}{\partial t^2} = 0, \tag{24a}$$

$$-\frac{\partial N_{x2}}{\partial x} + \rho_t A_2 \frac{\partial^2 u_2}{\partial t^2} = 0, \tag{24b}$$

$$\begin{aligned} &-\frac{\partial}{\partial x}\left(N_{x1}\frac{\partial w_1}{\partial x}\right) - \frac{\partial^2 M_{x1}}{\partial x^2} + \rho_f A_f\left(2V_\infty \frac{\partial^2 w_1}{\partial x \partial t} + V_\infty^2 \frac{\partial^2 w_1}{\partial x^2}\right) - \left(\rho_t I_1 + \rho_f I_f\right)\frac{\partial^4 w_1}{\partial x^2 \partial t^2} \\ &+\left(\rho_t A_1 + \rho_f A_f\right)\frac{\partial^2 w_1}{\partial t^2} = -\rho_f A_f\left(\frac{\partial^2 w_1}{\partial t^2} + 2V_\infty \frac{\partial^2 w_1}{\partial x\,\partial t} + \frac{\partial u_1}{\partial t}\frac{\partial^2 w_1}{\partial x\,\partial t} + \frac{\partial u_1}{\partial t}V_\infty \frac{\partial^2 w_1}{\partial x^2} + V_\infty^2 \frac{\partial^2 w_1}{\partial x^2}\right) \\ &+\mu A_f \frac{\partial^3 w_1}{\partial x^2\,\partial t} + \mu A_f V_\infty \frac{\partial^3 w_1}{\partial x^3} + 2\pi R_{o1} c\left(w_2 - w_1\right), \end{aligned} \tag{24c}$$

$$\begin{aligned} &-\frac{\partial}{\partial x}\left(N_{x2}\frac{\partial w_2}{\partial x}\right) - \frac{\partial^2 M_{x2}}{\partial x^2} - \rho_t I_2 \frac{\partial^4 w_2}{\partial x^2 \partial t^2} + \rho_t A_2 \frac{\partial^2 w_2}{\partial t^2} = \\ &-2\pi R_{o2}\left(K_w w_2 - K_G \frac{\partial^2 w_2}{\partial x^2}\right) - 2\pi R_{o1} c\left(w_2 - w_1\right), \end{aligned} \tag{24d}$$

$$\int_{A_1} \frac{\partial D_{x1}}{\partial x} dA = 0, \tag{24e}$$

$$\int_{A_2} \frac{\partial D_{x2}}{\partial x} dA = 0. \tag{24f}$$

In above equations, I_1, I_2 and I_f are defined as:

$$I_i = \int_{A_i} z^2 dA, \quad i = 1,2 \tag{25a}$$

$$I_f = \int_{A_f} z^2 dA. \tag{25b}$$

Neglecting the effects of Pasternak foundation, electric loading and flowing fluid, Eqs. (24a)-(24d) reduces to the relations in [26].

© 2012 IAU, Arak Branch

www.SID.ir

Archive of SID

2.10 Eringen theory

Nonlocal elasticity theory is used in this study [11] , [21]. Eringen's theory for the Euler beam under combined loading is expressed as [19] :

$$\sigma_{xi}-\left(e_0a\right)^2\frac{\partial^2\sigma_{xi}}{\partial x^2}=E\left(\frac{\partial u_i}{\partial x}+\frac{1}{2}\left(\frac{\partial w_i}{\partial x}\right)^2-z\frac{\partial^2 w_i}{\partial x^2}-\alpha_x T\right)-h_{11}E_{xi}, \tag{26}$$

where E,α_x,T and h_{11} represent the Young modulus, thermal expansion coefficient, thermal changes and piezoelectric coefficient respectively. Considering the definitions of N_{xi} and M_{xi} (as mentioned in section 2-3), Eq. (26) results in:

$$N_{xi}-\left(e_0a\right)^2\frac{\partial^2 N_{xi}}{\partial x^2}=EA_i\left(\frac{\partial u_i}{\partial x}+\frac{1}{2}\left(\frac{\partial w_i}{\partial x}\right)^2-\alpha_x T\right)-h_{11}E_{xi}A_i, \tag{27}$$

$$M_{xi}-\left(e_0a\right)^2\frac{\partial^2 M_{xi}}{\partial x^2}=-EI_i\frac{\partial^2 w_i}{\partial x^2} \tag{28}$$

A combination of electro-thermo mechanical loading is exerted on the DWBNNT, so according to [18]:

$$N_{xi}=N_{xi}^M+N_{xi}^T+N_{xi}^E, \tag{29}$$

where superscript M,T and E indicate mechanical, thermal and electrical components of load as:

$$N_{xi}^T=-EA_i\alpha_x T, \tag{30a}$$

$$N_{xi}^E=-h_{11}E_{xi}A_i, \tag{30b}$$

$$N_{xi}^M=N_0+N_s\cos\left(pt\right), \tag{30c}$$

where p represents the frequency of the applied excitation [24], N_0 is the static component of N^M and N_s is the dynamic load amplitude, which may be expressed as:

$$N_0=a_1N_{cr}, \tag{31a}$$

$$N_s=a_2N_{cr}. \tag{31b}$$

In above Eqs. a_1 and a_2 are the static and dynamic load factors, respectively and N_{cr} is the static load buckling [2]. In Eqs. (27) and (28), 2nd derivatives of N_{xi} and M_{xi} can be evaluated from Eq. (24), so Eqs. (27) - (28) can be arranged as:

$$N_{x1}=EA_1\frac{\partial u_1}{\partial x}+\frac{1}{2}EA_1\left(\frac{\partial w_1}{\partial x}\right)^2-EA_1\alpha_x T-h_{11}E_{x1}A_1+\left(e_0a\right)^2\rho_tA_1\frac{\partial^3 u_1}{\partial x\,\partial t^2}+\left(e_0a\right)^2\rho_fA_f\frac{\partial^3 u_1}{\partial x\,\partial t^2} \tag{32a}$$

© 2012IAU, Arak Branch

Archive of SID

www.SID.ir

$$N_{x2} = EA_2 \frac{\partial u_2}{\partial x} + \frac{1}{2} EA_2 \left(\frac{\partial w_2}{\partial x} \right)^2 - EA_2 \alpha_x T - h_{11} E_{x2} A_1 + (e_0 a)^2 \rho_t A_2 \frac{\partial^3 u_2}{\partial x \partial t^2} \tag{32b}$$

$$\begin{aligned} M_{x1} &= -EI_1 \frac{\partial^2 w_1}{\partial x^2} + 2(e_0 a)^2 \rho_f A_f V \frac{\partial^2 w_1}{\partial x \partial t} + (e_0 a)^2 (\rho_t A_1 + \rho_f A_f) \frac{\partial^2 w_1}{\partial t^2} \\ &- (e_0 a)^2 \mu A_f \left(V \frac{\partial^3 w_1}{\partial x^3} + \frac{\partial^3 w_1}{\partial x^2 \partial t} \right) + (e_0 a)^2 \left(EA_1 \alpha_x T - N_{x1}^M - h_{11} A_1 \frac{\partial \Phi_1}{\partial x} \right) \frac{\partial^2 w_1}{\partial x^2} \\ &- (e_0 a)^2 h_{11} A_1 \frac{\partial w_1}{\partial x} \frac{\partial^2 \Phi_1}{\partial x^2} - (e_0 a)^2 (\rho_f I_f + \rho_t I_1) \frac{\partial^4 w_1}{\partial x^2 \partial t^2} - 2\pi R_{o1} c (e_0 a)^2 (w_2 - w_1) \\ &+ (e_0 a)^2 \rho_f A_f \left(\frac{\partial^2 w_1}{\partial t^2} + 2V_\infty \frac{\partial^2 w_1}{\partial x \partial t} + \frac{\partial u_1}{\partial t} \frac{\partial^2 w_1}{\partial x \partial t} + V_\infty \frac{\partial u_1}{\partial t} \frac{\partial^2 w_1}{\partial x^2} + 2V_\infty^2 \frac{\partial^2 w}{\partial x^2} \right) \end{aligned} \tag{32c}$$

$$\begin{aligned} M_{x2} &= -EI_2 \frac{\partial^2 w_2}{\partial x^2} + (e_0 a)^2 \rho_t A_2 \frac{\partial^2 w_2}{\partial t^2} - (e_0 a)^2 \rho_t I_2 \frac{\partial^4 w_2}{\partial x^2 \partial t^2} \\ &+ (e_0 a)^2 \left(EA_2 \alpha_x T - N_{x2}^M - h_{11} A_2 \frac{\partial \Phi_2}{\partial x} \right) \frac{\partial^2 w_2}{\partial x^2} - (e_0 a)^2 h_{11} A_2 \frac{\partial w_2}{\partial x} \frac{\partial^2 \Phi_2}{\partial x^2} \\ &+ 2\pi R_{o1} c (e_0 a)^2 (w_2 - w_1) + 2\pi R_{o2} (e_0 a)^2 \left(K_w w_2 - K_G \frac{\partial^2 w_2}{\partial x^2} \right) \end{aligned} \tag{32d}$$

Final equations of motion can be derived by substituting Eqs. (32a) – (32d) into Eq. (24a) - (24d) as following:

$$\begin{aligned} &-EA_1 \frac{\partial^2 u_1}{\partial x^2} - EA_1 \frac{\partial w_1}{\partial x} \frac{\partial^2 w_1}{\partial x^2} - h_{11} A_1 \frac{\partial^2 \Phi_1}{\partial x^2} - (e_0 a)^2 \rho_t A_1 \frac{\partial^4 u_1}{\partial x^2 \partial t^2} \\ &- (e_0 a)^2 \rho_f A_f \frac{\partial^4 u_1}{\partial x^2 \partial t^2} + \rho_t A_1 \frac{\partial^2 u_1}{\partial t^2} + \rho_f A_f \frac{\partial^2 u_1}{\partial t^2} = 0, \end{aligned} \tag{33a}$$

$$-EA_2 \frac{\partial^2 u_2}{\partial x^2} - EA_2 \frac{\partial w_2}{\partial x} \frac{\partial^2 w_2}{\partial x^2} - h_{11} A_2 \frac{\partial^2 \Phi_2}{\partial x^2} - (e_0 a)^2 \rho_t A_2 \frac{\partial^4 u_2}{\partial x^2 \partial t^2} + \rho_t A_1 \frac{\partial^2 u_1}{\partial t^2} = 0, \tag{33b}$$

$$\begin{aligned} &-\left(N_M + h_{11} A_1 \frac{\partial \Phi_1}{\partial x} - EA_1 \alpha_x T \right) \frac{\partial^2 w_1}{\partial x^2} - h_{11} A_1 \frac{\partial^2 \Phi_1}{\partial x^2} \frac{\partial w_1}{\partial x} + EI_1 \frac{\partial^4 w_1}{\partial x^4} - 2(e_0 a)^2 \rho_f A_f V \frac{\partial^4 w_1}{\partial x^3 \partial t} \\ &- (e_0 a)^2 (\rho_t A_1 + \rho_f A_f) \frac{\partial^4 w_1}{\partial x^2 \partial t^2} + (e_0 a)^2 \mu A_f \left(V \frac{\partial^5 w_1}{\partial x^5} + \frac{\partial^5 w_1}{\partial x^4 \partial t} \right) + (e_0 a)^2 \left(N_M + h_{11} A_1 \frac{\partial \Phi_1}{\partial x} - EA_1 \alpha_x T \right) \frac{\partial^4 w_1}{\partial x^4} \\ &+ (e_0 a)^2 h_{11} A_1 \left(\frac{\partial^3 \Phi_1}{\partial x^3} \frac{\partial^2 w_1}{\partial x^2} + 2 \frac{\partial^2 \Phi_1}{\partial x^2} \frac{\partial^3 w_1}{\partial x^3} \right) + h_{11} A_1 (e_0 a)^2 \left(\frac{\partial^3 w_1}{\partial x^3} \frac{\partial^2 \Phi_1}{\partial x^2} + 2 \frac{\partial^2 w_1}{\partial x^2} \frac{\partial^3 \Phi_1}{\partial x^3} + \frac{\partial w_1}{\partial x} \frac{\partial^4 \Phi_1}{\partial x^4} \right) \\ &- (e_0 a)^2 \rho_f A_f \left(\frac{\partial^4 w_1}{\partial x^2 \partial t^2} + 2V_\infty \frac{\partial^4 w_1}{\partial x^3 \partial t} + \frac{\partial^3 u_1}{\partial x^2 \partial t} \frac{\partial^2 w_1}{\partial x \partial t} + \frac{\partial u_1}{\partial t} \frac{\partial^4 w_1}{\partial x^3 \partial t} + V_\infty \frac{\partial u_1}{\partial t} \frac{\partial^4 w_1}{\partial x^4} + V_\infty \frac{\partial^3 u_1}{\partial x^2 \partial t} \frac{\partial^2 w_1}{\partial x^2} + 2V_\infty^2 \frac{\partial^4 w_1}{\partial x^4} \right) \\ &+ (e_0 a)^2 (\rho_t I_1 + \rho_f I_f) \frac{\partial^6 w_1}{\partial x^4 \partial t^2} - (e_0 a)^2 \rho_f A_f \left(2V \frac{\partial^2 u_1}{\partial x \partial t} \frac{\partial^3 w_1}{\partial x^3} + 2 \frac{\partial^2 u_1}{\partial x \partial t} \frac{\partial^3 w_1}{\partial x^2 \partial t} \right) + 2\pi R_{o1} (e_0 a)^2 c \left(\frac{\partial^2 w_2}{\partial x^2} - \frac{\partial^2 w_1}{\partial x^2} \right) \\ &- (\rho_t I_1 + \rho_f I_f) \frac{\partial^4 w_1}{\partial x^2 \partial t^2} + (\rho_t A_1 + \rho_f A_f) \frac{\partial^2 w_1}{\partial t^2} + \rho_f A_f \left(2V_\infty \frac{\partial^2 w_1}{\partial x \partial t} + V_\infty^2 \frac{\partial^2 w_1}{\partial x^2} \right) \\ &= -\rho_f A_f \left(\frac{\partial^2 w_1}{\partial t^2} + 2V_\infty \frac{\partial^2 w_1}{\partial x \partial t} + V_\infty \frac{\partial u_1}{\partial t} \frac{\partial^2 w_1}{\partial x^2} + \frac{\partial u_1}{\partial t} \frac{\partial^2 w_1}{\partial x \partial t} + V_\infty^2 \frac{\partial^2 w_1}{\partial x^2} \right) + \mu A_f \left(\frac{\partial^3 w_1}{\partial x^2 \partial t} + V_\infty \frac{\partial^3 w_1}{\partial x^3} \right) + 2\pi R_{o1} c (w_2 - w_1), \end{aligned} \tag{33c}$$

© 2012 IAU, Arak Branch

www.SID.ir

Archive of SID

$$
\begin{aligned}
&-\left(N_M + h_{11}A_2\frac{\partial\Phi_2}{\partial x} - EA_2\alpha_x T\right)\frac{\partial^2 w_2}{\partial x^2} - h_{11}A_2\frac{\partial^2\Phi_2}{\partial x^2}\frac{\partial w_2}{\partial x} + EI_2\frac{\partial^4 w_2}{\partial x^4}\\
&-\rho_t A_2\left(e_0 a\right)^2\frac{\partial^4 w_2}{\partial x^2\partial t^2} + \left(e_0 a\right)^2\left(N_M + h_{11}A_2\frac{\partial\Phi_2}{\partial x} - EA_2\alpha_x T\right)\frac{\partial^4 w_2}{\partial x^4}\\
&+h_{11}A_2\left(e_0 a\right)^2\left(3\frac{\partial^3 w_2}{\partial x^3}\frac{\partial^2\Phi_2}{\partial x^2} + 3\frac{\partial^2 w_2}{\partial x^2}\frac{\partial^3\Phi_2}{\partial x^3} + \frac{\partial w_2}{\partial x}\frac{\partial^4\Phi_2}{\partial x^4}\right)\\
&-\rho_t I_2\frac{\partial^4 w_2}{\partial x^2\partial t^2} + \rho_t A_2\frac{\partial^2 w_2}{\partial t^2} - 2\left(e_0 a\right)^2\pi R_{2o}\left(K_w\frac{\partial^2 w_2}{\partial x^2} - K_G\frac{\partial^4 w_2}{\partial x^4}\right)\\
&-2\left(e_0 a\right)^2 c\pi R_{o1}\left(\frac{\partial^2 w_2}{\partial x^2} - \frac{\partial^2 w_1}{\partial x^2}\right) + \rho_t I_2\left(e_0 a\right)^2\frac{\partial^6 w_2}{\partial x^4\partial t^2}\\
&= -2\pi\left(R_{o2}K_w w_2 - R_{o2}K_G\frac{\partial^2 w_2}{\partial x^2} + cR_{o1}w_2 - cR_{o1}w_1\right).
\end{aligned}
\tag{33d}
$$

Electrical – mechanical coupling is expressed as following according to the [27], [19]:

$$D_x = \zeta\varepsilon_x + h_{11}E_x, \tag{34}$$

where ζ is the dielectric permittivity. Hence, Eqs. (24e) and (24f) can be changed as below:

$$-\zeta\frac{\partial^2\Phi_2}{\partial x^2} + h_{11}\left(\frac{\partial^2 u_2}{\partial x^2} + \frac{\partial w_2}{\partial x}\frac{\partial^2 w_2}{\partial x^2}\right) = 0. \tag{35a}$$

$$-\zeta\frac{\partial^2\Phi_1}{\partial x^2} + h_{11}\left(\frac{\partial^2 u_1}{\partial x^2} + \frac{\partial w_1}{\partial x}\frac{\partial^2 w_1}{\partial x^2}\right) = 0, \tag{35b}$$

In this study, the following dimensionless groups are used :

$$
\begin{aligned}
&T = \frac{t}{L}\sqrt{\frac{E}{\rho_t}},\quad X = \frac{x}{L},\quad \alpha = \frac{e_0 a}{L},\quad A_n = \frac{A_f}{L^2},\quad A_{n1} = \frac{A_1}{L^2},\quad A_{n2} = \frac{A_2}{L^2},\quad \rho = \frac{\rho_f}{\rho_t},\\
&\left(\Phi_{n1},\Phi_{n2}\right) = \left(\frac{\Phi_1 h_{11}}{EL},\frac{\Phi_2 h_{11}}{EL}\right),\quad v = V_\infty\sqrt{\frac{\rho_t}{E}},\quad \left(R_{n1},R_{n2},R_{no1},R_{no2}\right) = \frac{\left(R_1,R_2,R_{o1},R_{o2}\right)}{L},\\
&\left(U_1,U_2\right) = \frac{\left(u_1,u_2\right)}{L},\quad \left(I,I_{n1},I_{n2}\right) = \frac{\left(I_f,I_1,I_2\right)}{L^4},\quad \mu_n = \frac{\mu}{L\rho_t V_\infty},\quad C = \frac{cL}{E},\quad K_{nw} = \frac{K_w L}{E},\\
&K_{nG} = \frac{K_G}{EL},\quad \Delta = \alpha_x T,\quad \left(W_1,W_2\right) = \frac{\left(w_1,w_2\right)}{h},\quad \beta = \frac{h}{L},\quad H = \frac{h_{11}^2}{E\zeta},\quad N_M = \frac{N_{xi}^M}{EA_1}.
\end{aligned}
\tag{36}
$$

So non-dimension motion equations can be derived by substituting Eq. (36) into Eqs. (33a) – (33d) and (35a) – (35b) as presented in Appendix A.

3 DIFFERENTIAL QUADRATURE METHOD

This method is based on Gauss approximation. *N* point are selected as discrete points in the domain using Cheybeshev approximation as follows:

© 2012IAU, Arak Branch

Archive of SID

www.SID.ir

$$X_j = \frac{1}{2}\left\{1-\cos\left[\frac{\pi(j-1)}{N-1}\right]\right\} \quad j=1,2,...,N. \tag{37}$$

According to this method, the functions U_i, W_i, Φ_{ni} and their derivatives are approximated as [13],[28]:

$$\{U_i, W_i, \Phi_{ni}\} = \sum_{m=1}^{N} l_m(X)\{U_{im}(X,T), W_{im}(X,T), \Phi_i(X)\}, \quad i=1,2 \tag{38}$$

$$\frac{\partial^k}{\partial x^k}\{U_i, W_i, \Phi_{ni}\} = \sum_{m=1}^{N} C_{jm}^{(k)}(X)\{U_{im}(X,T), W_{im}(X,T), \Phi_{im}(X)\}, \quad i=1,2 \tag{39}$$

where $l_m(X)$ and $C_{jm}^{(k)}$ represent the Lagrange interpolation polynomial and it's k^{th} derivative, that can be found in [28]. Implying this method to equations of Appendix A, a set of ordinary differential equations can be derived which are presented in Appendix B, where derivatives with respect to dimensionless time are shown with dot. In this study the boundary condition of DWBNNT is clamped-clamped that can be stated as :

$$\begin{aligned} &W_{i1} = U_{i1} = 0, \quad \sum_{m=1}^{N} C_{2m}^{(1)} W_{im}, \quad i=1,2 \\ &W_{iN} = U_{iN} = 0, \quad \sum_{m=1}^{N} C_{N-1m}^{(1)} W_{im}, \quad i=1,2 \end{aligned} \tag{40}$$

Equations of Appendix B can be arranged in the matrix form as:

$$\left(K_L + K_{NL} - \left(a_1 P_{cr} + a_2 P_{cr}\cos(pt)\right)\left(K_L' + K_{NL}'\right)\right)d + \left(C_L + C_{NL}\right)\dot{d} + \left(M_L + M_{NL}\right)\ddot{d} = 0, \tag{41}$$

where K, K', C and M are the stiffness, geometric, damping and mass matrixes, L and NL indexes indicate linear and nonlinear terms [28] and d is the defined as:

$$d = \begin{Bmatrix} d_a \\ d_b \end{Bmatrix}, \tag{42}$$

In above equation, subscript b denotes boundary points and other points are indicated by subscript a as:

$$\begin{aligned} &d_a = \left\{U_{i3},...,U_{iN-2}, W_{i3},...,W_{iN-2}, \Phi_{i3},...,\Phi_{iN-2}\right\}^T, \quad i=1,2 \\ &d_b = \left\{U_{i1}, U_{i2}, U_{iN-1}, U_{iN}, W_{i1}, W_{i2}, W_{iN-1}, W_{iN}, \Phi_{i1}, \Phi_{i2}, \Phi_{iN-1}, \Phi_{iN}\right\}^T. \quad i=1,2 \end{aligned} \tag{43}$$

Solving Eq. (41) results the dynamic load factor (a_2) as stated in the next section.

4 NUMERICAL RESULTS

The final converged solutions using the numerical procedure outlined in section 3 above (with 15 grid points in length direction of beam) are illustrated as effects of buckling modes, small scale parameters, elastic medium, temperature changes, fluid velocity and frequency on dimensionless dynamic buckling load. All calculations are

© 2012 IAU, Arak Branch

www.SID.ir

Archive of SID

performed for a beam having the following geometrical parameters: $R_1 = 11.43\,nm$, $R_2 = 12.31\,nm$, $L = 10 \times R_1$ and $h = 0.075\,nm$ which indicate the inner radius, outer radius, length and thickness of DWBNNT, respectively. The mechanical, thermal and electrical characteristics of DWBNNT are $E = 1.8\,Tpa$, $\rho_t = 2300\ kg/m^3$, $K_G = 2.071273\ N/m$, $K_w = 8.9995035 \times 10^{17}\ N/m^3$, $c = 9.91866693 \times 10^{19}\ N/m^3$, $\alpha_x = 1.2 \times 10^{-6}\,1/K$, $h_{11} = 0.95C/m^2$ and $\zeta = 0.9824 \times 10^{-8}\ F/m$ which represent elastic modulus, mass density, Pasternak and Winkler spring constants of elastic medium, vdW coefficient, thermal expansion coefficient, piezoelectric coefficient and dielectric permittivity, respectively [17, 21]. In order to analyze the effect of flow velocity on the response frequency of the DWBNNT, we assumed that the flowing liquid is water and its mass density and viscosity are $1000\ kg/m^3$ and $1.12 \times 10^{-3}\ Pa.s$ [19,21].

In the absence of similar publications in the literature covering the same scope of the problem, one can not directly validate the results found here. However, the present work could be partially validated based on a simplified analysis suggested by Ansari et al. [29]. On the dynamic stability of embedded single-walled CNTs for which the electric field and vdW force in this paper were ignored. For this purpose, a single-walled CNT with $E = 1.1\,\text{TPa}$, $\rho = 1300\ \text{Kg/m}^3$, $d = 3\ \text{nm}$, $t = 0.34\ \text{nm}$ and $T = 50\ ^0K$ was considered. The results of validation are shown in Fig. 2 in which dynamic buckling load factor versus frequency for different nonlocal parameter is plotted. As can be seen the two analyses agree well and show similar results.

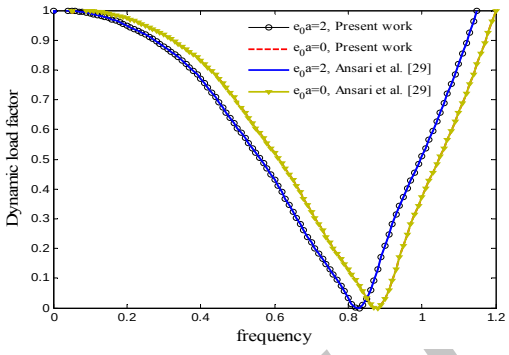

Fig.2
Dimensionless dynamic buckling load factor versus frequency for different nonlocal parameter.

Figs. 3-7 show the dynamic load factor versus non-dimensional time. Generally, with increasing the non-dimensional time the dynamic buckling load sharply decreases and becomes asymptotic with the horizontal axis.

Fig. 3 represents the effect of nonlocal parameter on the dynamic load factor versus dimensionless time. It shows that the nonlocal effect decreases the dynamic buckling load. So the classical continuum model ($\alpha = 0$), predicts higher dynamic buckling load than the nonlocal model. It is perhaps due to the fact that increasing the nonlocal parameter results in $B-N$ bond elongation, so less dynamic buckling load is required for DWBNNT buckling.

Fig. 4 shows the effect of temperature changes on dynamic load factor versus dimensionless time. As can be seen with increasing the temperature change results in less dynamic buckling load. It is perhaps due to increasing temperature change will weaken the $B-N$ bond and subsequently makes the DWBNNT softer.

The effect of Pasternak foundation on dynamic load factor versus dimensionless time is represented in Fig. 5. The obtained results show that the dynamic buckling load increases with increasing Pasternak shear modulus. This is because increasing Pasternak coefficient increases the DWBNNT stiffness.

Fig. 6 shows the dynamic load factor versus dimensionless time in different buckling modes. The least buckling load is related to the first mode and the dynamic buckling load will rise as the mode number increases.

Fig. 7 indicates the effect of geometrical parameter of DWBNNT (i.e. thickness to length ratio (β)) on dynamic load factor versus dimensionless time. It is observed that increasing β results in higher dynamic buckling load; because DWBNNT becomes stiffer and more dynamic buckling load is required.

Archive of SID

© 2012IAU, Arak Branch

www.SID.ir

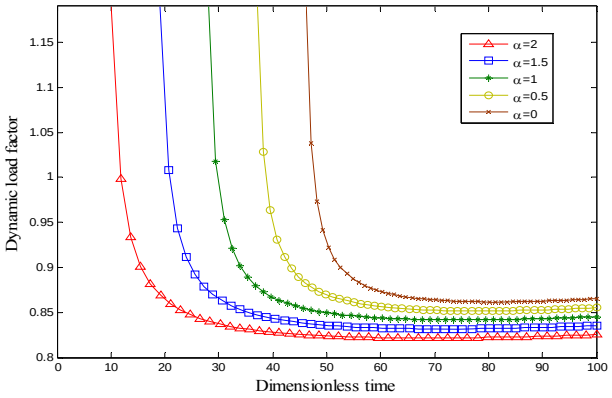

Fig.3
Dimensionless dynamic buckling load factor versus dimensionless time, the effect of nonlocal parameter.

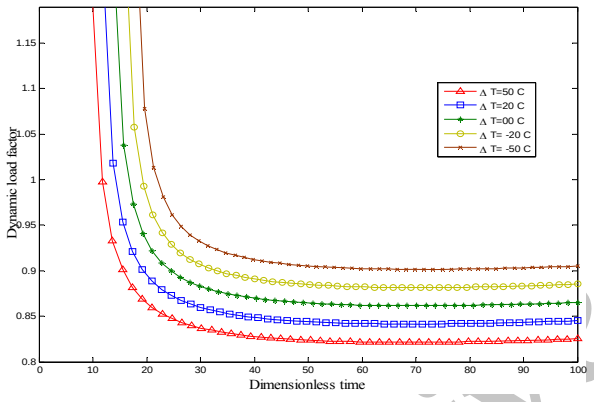

Fig.4
Dimensionless dynamic buckling load factor versus dimensionless time, the effect of thermal changes.

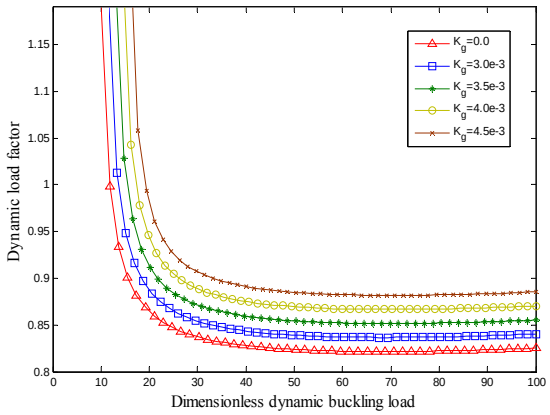

Fig.5
Dimensionless dynamic buckling load factor versus dimensionless time, the effect of Pasternak medium.

© 2012 IAU, Arak Branch

www.SID.ir

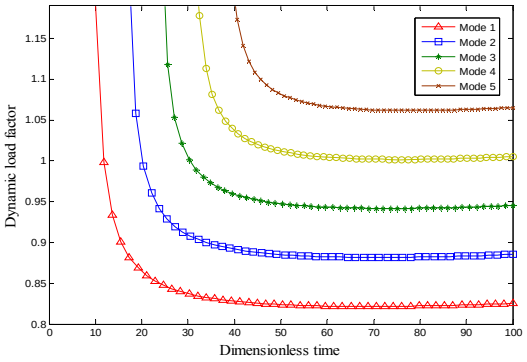

Fig.6
Dimensionless dynamic buckling load factor versus dimensionless time, the effect of buckling mode.

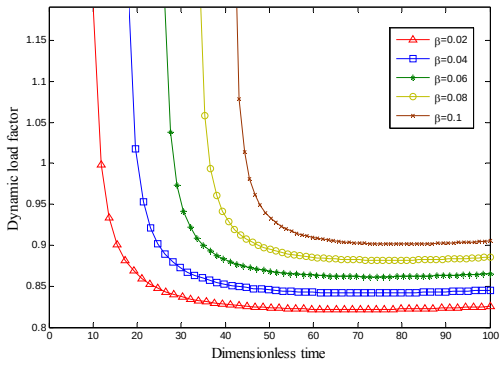

Fig.7
Dimensionless dynamic buckling load factor versus dimensionless time, the effect of parameter β.

In Figs. 8-10 dynamic load factor is plotted versus dimensionless frequency. These figures indicate the dynamic stability of DWBNNT. Generally, as dimensionless frequency increases, dynamic buckling loads decrease sharply first to a minimum, before they increase sharply again.

The effect of nonlocal parameter on dynamic load factor versus dimensionless frequency is represented in Fig. 8. It's observed that dynamic instability region (DIR) is at higher frequency for the local model. Increasing the nonlocal parameter shifts the instability zone to the lower frequency.

Fig. 9 shows the effect of fluid velocity on dynamic load factor versus dimensionless frequency. It's observed that increasing the fluid velocity in DWBNNT shifts the DIR to the lower frequency zone so DWBNNT is more stable when the velocity of fluid is zero.

Fig 10 indicates dynamic load factor versus dimensionless frequency for different buckling modes. As can be seen, the DIR is at the minimum frequency zone for the first mode and with increasing mode number shifts to the higher frequencies.

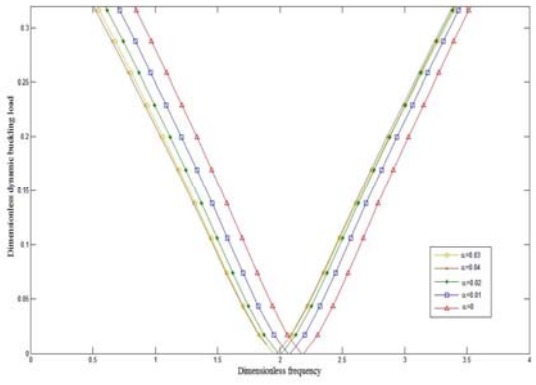

Fig.8
The effect of nonlocal parameter on DIR.

Archive of SID

© 2012IAU, Arak Branch

www.SID.ir

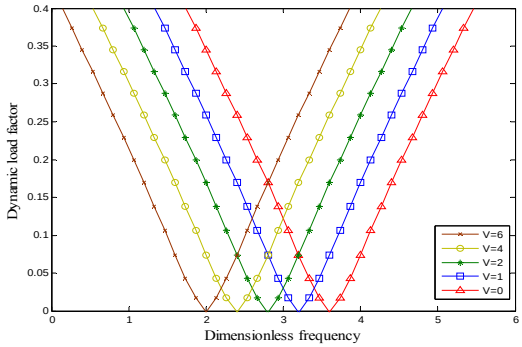

Fig.9
The effect of fluid velocity on DIR.

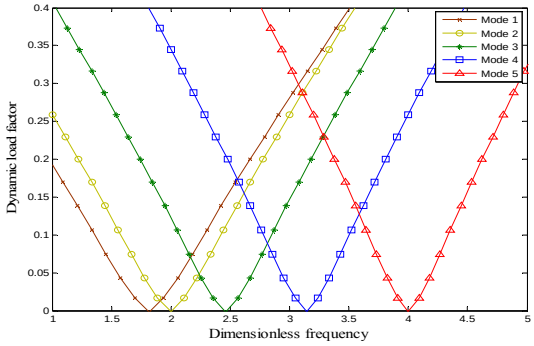

Fig.10
The effect of buckling mode on DIR.

Archive of SID

5 CONCLUSIONS

Applying DQM and considering charge equation, nonlocal nonlinear dynamic buckling of embedded DWBNNTs conveying viscous fluid was investigated using Euler-Bernoulli beam theory. The effects of the surrounding elastic medium, such as the shear constant of the Pasternak type as well as the vdW forces between the inner and outer nanotubes were taken into account. The following conclusions may be made from the results:

- Nonlocal continuum model predicts lower dynamic buckling load than the classical one.
- Dynamic buckling load is increased when the thermal changes are reduced.
- DWBNNT embedded in a stiffer medium buckles at higher dynamic buckling load.
- Dynamic instability region occurs at higher frequency zone when the nonlocal Eringen's theory is implied.
- Dynamic instability region occurs at lower frequency zone by increasing the velocity of flowing fluid in DWBNNT.

ACKNOWLEDGMENTS

The authors are grateful to University of Kashan for supporting this work by Grant No. 65475/33. They would also like to thank the Iranian Nanotechnology Development Committee for their financial support. This research was supported by the Thermoelasticity Center of Excellence, Mechanical Engineering Department, Amirkabir University of Technology.

© 2012 IAU, Arak Branch

www.SID.ir

APPENDIX A

$$\frac{\partial^2 U_1}{\partial X^2}+\beta^2\frac{\partial W_1}{\partial X}\frac{\partial^2 W_1}{\partial X^2}+\frac{\partial^2 \Phi_{n1}}{\partial x^2}+\alpha^2\frac{\partial^4 U_1}{\partial X^2\partial T^2}+\frac{\alpha^2\rho A_n}{A_{n1}}\frac{\partial^4 U_1}{\partial X^2\partial T^2}-\frac{\partial^2 U_1}{\partial T^2}-\frac{\rho A_n}{A_{n1}}\frac{\partial^2 U_1}{\partial T^2}=0, \tag{A1}$$

$$\frac{\partial^2 U_2}{\partial X^2}+\beta^2\frac{\partial W_2}{\partial X}\frac{\partial^2 W_2}{\partial X^2}+\frac{\partial^2 \Phi_{n2}}{\partial x^2}+\alpha^2\frac{\partial^4 U_2}{\partial X^2\partial T^2}-\frac{\partial^2 U_2}{\partial T^2}=0, \tag{A2}$$

$$\begin{aligned}
&+\beta\left(N_M+\frac{\partial\Phi_{n1}}{\partial X}-\Delta\right)\frac{\partial^2 W_1}{\partial X^2}+\beta\frac{\partial W_1}{\partial X}\frac{\partial^2\Phi_{n1}}{\partial X^2}-\frac{I_{n1}\beta}{A_{n1}}\frac{\partial^4 W_1}{\partial X^4}+\frac{2\alpha^2\beta\rho A_n\nu}{A_{n1}}\frac{\partial^4 W_1}{\partial X^3\partial T}\\
&+\alpha^2\beta\left(1+\frac{\rho A_n}{A_{n1}}\right)\frac{\partial^4 W_1}{\partial X^2\partial T^2}-\frac{\alpha^2\beta\mu_n\nu A_n}{A_{n1}}\left(\frac{\partial^5 W_1}{\partial X^4\partial T}+\nu\frac{\partial^5 W_1}{\partial X^5}\right)-\alpha^2\beta\left(N_M+\frac{\partial\Phi_{n1}}{\partial X}-\Delta\right)\frac{\partial^4 W_1}{\partial X^4}\\
&-\alpha^2\beta\left(\frac{\partial^3\Phi_{n1}}{\partial X^3}\frac{\partial^2 W_1}{\partial X^2}+2\frac{\partial^2\Phi_{n1}}{\partial X^2}\frac{\partial^3 W_1}{\partial X^3}\right)-\alpha^2\beta\left(\frac{\partial^3 W_1}{\partial X^3}\frac{\partial^2\Phi_{n1}}{\partial X^2}+2\frac{\partial^2 W_1}{\partial X^2}\frac{\partial^3\Phi_{n1}}{\partial X^3}+\frac{\partial W_1}{\partial X}\frac{\partial^4\Phi_{n1}}{\partial X^4}\right)\\
&-\alpha^2\beta\left(\frac{\rho I}{A_{n1}}+\frac{I_{n1}}{A_{n1}}\right)\frac{\partial^6 W_1}{\partial X^4\partial T^2}+\frac{\alpha^2\beta\rho A_n}{A_{n1}}\left(\frac{\partial^4 W_1}{\partial X^2\partial T^2}+2\nu\frac{\partial^4 W_1}{\partial X^3\partial T}+\frac{\partial^3 U_1}{\partial X^2\partial T}\frac{\partial^2 W_1}{\partial X\partial T}\right.\\
&\left.\frac{\partial U_1}{\partial T}\frac{\partial^4 W_1}{\partial X^3\partial T}+\nu\frac{\partial U_1}{\partial T}\frac{\partial^4 W_1}{\partial X^4}+\nu\frac{\partial^3 U_1}{\partial X^2\partial T}\frac{\partial^2 W_1}{\partial X^2}+2\nu^2\frac{\partial^4 W_1}{\partial X^4}+2\nu\frac{\partial^2 U_1}{\partial X\partial T}\frac{\partial^3 W_1}{\partial X^3}\right)+\frac{2\alpha^2\beta\rho A_n}{A_{n1}}\frac{\partial^2 U_1}{\partial X\partial T}\frac{\partial^3 W_1}{\partial X^2\partial T}\\
&+\frac{2\pi R_{no1}\alpha^2\beta C}{A_{n1}}\left(\frac{\partial^2 W_1}{\partial X^2}-\frac{\partial^2 W_2}{\partial X^2}\right)+\frac{\beta}{A_{n1}}(\rho I+I_{n1})\frac{\partial^4 W_1}{\partial X^2\partial T^2}-\left(1+\frac{\rho A_n}{A_{n1}}\right)\beta\frac{\partial^2 W_1}{\partial T^2}\\
&-\frac{\beta\rho A_n}{A_{n1}}\left(\frac{2\nu\partial^2 W_1}{\partial X\partial T}+\nu^2\right)\frac{\partial^2 W_1}{\partial X^2}=\frac{\rho A_n\beta}{A_{n1}}\frac{\partial^2 W_1}{\partial T^2}+\frac{\beta\rho A_n}{A_{n1}}\left(2\nu\frac{\partial^2 W_1}{\partial X\partial T}+\nu\frac{\partial U_1}{\partial T}\frac{\partial^2 W_1}{\partial X^2}+\frac{\partial U_1}{\partial T}\frac{\partial^2 W_1}{\partial X\partial T}+\nu^2\frac{\partial^2 W_1}{\partial X^2}\right)\\
&-\frac{\beta\mu_n A_n}{A_{n1}}\left(\frac{\partial^3 W_1}{\partial X^2\partial T}+\nu\frac{\partial^3 W_1}{\partial X^3}\right)-\frac{2\pi R_{no1}C\beta}{A_{n1}}(W_2-W_1)
\end{aligned} \tag{A3}$$

$$\begin{aligned}
&\left(+\frac{A_{n1}N_M}{A_{n2}}+\frac{\partial\Phi_{n2}}{\partial X}-\Delta\right)\beta\frac{\partial^2 W_2}{\partial X^2}+\beta\frac{\partial^2\Phi_2}{\partial X^2}\frac{\partial W_2}{\partial X}-\frac{I_{n2}\beta}{A_{n2}}\frac{\partial^4 W_2}{\partial X^4}+\alpha^2\beta\frac{\partial^4 W_2}{\partial X^2\partial T^2}\\
&-\left(\frac{A_{n1}N_M}{A_{n2}}+\frac{\partial\Phi_2}{\partial X}-\Delta\right)\alpha^2\beta\frac{\partial^4 W_2}{\partial X^4}-\alpha^2\beta\left(3\frac{\partial^3 W_2}{\partial X^3}\frac{\partial^2\Phi_{n2}}{\partial X^2}+3\frac{\partial^2 W_2}{\partial X^2}\frac{\partial^3\Phi_2}{\partial X^3}+\frac{\partial W_2}{\partial X}\frac{\partial^4\Phi_{n2}}{\partial X^4}\right)
\end{aligned} \tag{A4}$$

$$\begin{aligned}
&+\frac{I_{n2}\beta}{A_{n2}}\frac{\partial^4 W_2}{\partial X^2\partial T^2}-\beta\frac{\partial^2 W_2}{\partial T^2}+\frac{2\alpha^2\beta\pi R_{no2}}{A_{n2}}\left(K_{nw}\frac{\partial^2 W_2}{\partial X^2}-K_{nG}\frac{\partial^4 W_2}{\partial X^4}\right)+\frac{2\alpha^2\beta C\pi R_{no1}}{A_{n2}}\left(\frac{\partial^2 W_2}{\partial X^2}-\frac{\partial^2 W_1}{\partial X^2}\right)\\
&-\frac{I_{n2}\alpha^2\beta}{A_{n2}}\frac{\partial^6 W_2}{\partial X^4\partial T^2}=+\frac{2\pi R_{no2}\beta}{A_{n2}}\left(K_{nw}W_2-K_{nG}\frac{\partial^2 W_2}{\partial X^2}\right)+\frac{2\pi C\beta R_{no1}}{A_{n2}}(W_2-W_1)
\end{aligned} \tag{A5}$$

$$\begin{aligned}
&\frac{\partial^2\Phi_{n1}}{\partial X^2}-H\frac{\partial^2 U_1}{\partial X^2}-H\beta^2\frac{\partial W_1}{\partial X}\frac{\partial^2 W_1}{\partial X^2}=0,\\
&\frac{\partial^2\Phi_{n2}}{\partial x^2}-H\frac{\partial^2 U_2}{\partial X^2}-H\beta^2\frac{\partial W_2}{\partial X}\frac{\partial^2 W_2}{\partial X^2}=0.
\end{aligned} \tag{A6}$$

© 2012IAU, Arak Branch

Archive of SID

www.SID.ir

APPENDIX B

$$\sum_{m=1}^{N} C_{jm}^{(2)} U_{1m} + \beta^2 \sum_{m=1}^{N} C_{jm}^{(1)} W_{1m} \sum_{m=1}^{N} C_{jm}^{(2)} W_{1m} + \sum_{m=1}^{N} C_{jm}^{(2)} \Phi_{1m} + \left(\alpha^2 + \frac{\alpha^2 \rho A_n}{A_{n1}} \right) \sum_{m=1}^{N} C_{jm}^{(2)} \ddot{U}_{1m} - \left(1 + \frac{\rho A_n}{A_{n1}} \right) \ddot{U}_{1j} = 0, \tag{B1}$$

$$\sum_{m=1}^{N} C_{jm}^{(2)} U_{2m} + \beta^2 \sum_{m=1}^{N} C_{jm}^{(1)} W_{2m} \sum_{m=1}^{N} C_{jm}^{(2)} W_{2m} + \sum_{m=1}^{N} C_{jm}^{(2)} \Phi_{2m} + \alpha^2 \sum_{m=1}^{N} C_{jm}^{(2)} \ddot{U}_{2m} - \ddot{U}_{2j} = 0, \tag{B2}$$

$$\begin{aligned}
&+\beta \left(N_M + \sum_{m=1}^{N} C_{jm}^{(1)} \Phi_{1m} - \Delta \right) \sum_{m=1}^{N} C_{jm}^{(2)} W_{1m} + \beta \sum_{m=1}^{N} C_{jm}^{(1)} W_{1m} \sum_{m=1}^{N} C_{jm}^{(2)} \Phi_{1m} - \frac{I_{n1} \beta}{A_{n1}} \sum_{m=1}^{N} C_{jm}^{(4)} W_{1m} + \frac{2\alpha^2 \beta \rho A_n \nu}{A_{n1}} \sum_{m=1}^{N} C_{jm}^{(3)} \dot{W}_{1m} \\
&+\alpha^2 \beta \left(1 + \frac{\rho A_n}{A_{n1}} \right) \sum_{m=1}^{N} C_{jm}^{(2)} \ddot{W}_{1m} - \frac{\alpha^2 \beta \mu_n \nu A_n}{A_{n1}} \left(\sum_{m=1}^{N} C_{jm}^{(4)} \dot{W}_{1m} + \nu \sum_{m=1}^{N} C_{jm}^{(5)} W_{1m} \right) - \alpha^2 \beta \left(N_M + \sum_{m=1}^{N} C_{jm}^{(1)} \Phi_{1m} - \Delta \right) \sum_{m=1}^{N} C_{jm}^{(4)} W_{1m} \\
&-\alpha^2 \beta \sum_{m=1}^{N} C_{jm}^{(3)} \Phi_{1m} \sum_{m=1}^{N} C_{jm}^{(2)} W_{1m} - 2\alpha^2 \beta \sum_{m=1}^{N} C_{jm}^{(2)} \Phi_{1m} \sum_{m=1}^{N} C_{jm}^{(3)} W_{1m} - \alpha^2 \beta \left(\sum_{m=1}^{N} C_{jm}^{(2)} \Phi_{1m} \sum_{m=1}^{N} C_{jm}^{(3)} W_{1m} \right. \\
&\left. +2 \sum_{m=1}^{N} C_{jm}^{(3)} \Phi_{1m} \sum_{m=1}^{N} C_{jm}^{(2)} W_{1m} + \sum_{m=1}^{N} C_{jm}^{(4)} \Phi_{1m} \sum_{m=1}^{N} C_{jm}^{(1)} W_{1m} \right) - \frac{\alpha^2 \beta}{A_{n1}} (\rho I + I_{n1}) \sum_{m=1}^{N} C_{jm}^{(4)} \ddot{W}_{1m} \\
&+\frac{\alpha^2 \beta \rho A_n}{A_{n1}} \left(\sum_{m=1}^{N} C_{jm}^{(2)} \ddot{W}_{1m} + 2\nu \sum_{m=1}^{N} C_{jm}^{(3)} \dot{W}_{1m} + \sum_{m=1}^{N} C_{jm}^{(2)} \dot{U}_{1m} \sum_{m=1}^{N} C_{jm}^{(1)} \dot{W}_{1m} + \dot{U}_{1j} \sum_{m=1}^{N} C_{jm}^{(3)} \dot{W}_{1m} + \nu \dot{U}_{1j} \sum_{m=1}^{N} C_{jm}^{(4)} W_{1m} \right) \\
&+\frac{\alpha^2 \beta \rho A_n}{A_{n1}} \left(\nu \sum_{m=1}^{N} C_{jm}^{(2)} \dot{U}_{1m} \sum_{m=1}^{N} C_{jm}^{(2)} W_{1m} + 2\nu^2 \sum_{m=1}^{N} C_{jm}^{(4)} W_{1m} + 2\nu \sum_{m=1}^{N} C_{jm}^{(1)} \dot{U}_{1m} \sum_{m=1}^{N} C_{jm}^{(3)} W_{1m} + 2 \sum_{m=1}^{N} C_{jm}^{(1)} \dot{U}_{1m} \sum_{m=1}^{N} C_{jm}^{(2)} \dot{W}_{1m} \right) \\
&+\frac{2\pi R_{no1} \alpha^2 \beta C}{A_{n1}} \left(\sum_{m=1}^{N} C_{jm}^{(2)} W_{1m} - \sum_{m=1}^{N} C_{jm}^{(2)} W_{2m} \right) + \frac{\beta}{A_{n1}} (\rho I + I_{n1}) \sum_{m=1}^{N} C_{jm}^{(2)} \ddot{W}_{1m} - \beta \left(1 + \frac{\rho A_n}{A_{n1}} \right) \ddot{W}_{1j} \\
&-\frac{\rho A_n \beta}{A_{n1}} \left(2\nu \sum_{m=1}^{N} C_{jm}^{(1)} \dot{W}_{1m} + \nu^2 \right) \sum_{m=1}^{N} C_{jm}^{(2)} W_{1m} = +\frac{\rho A_n \beta}{A_{n1}} \left(\ddot{W}_{1j} + 2\nu \sum_{m=1}^{N} C_{jm}^{(1)} \dot{W}_{1m} + \dot{U}_{1j} \sum_{m=1}^{N} C_{jm}^{(2)} W_{1m} + \nu^2 \sum_{m=1}^{N} C_{jm}^{(2)} W_{1m} \right) \\
&-\frac{\beta \mu_n A_n}{A_{n1}} \left(\sum_{m=1}^{N} C_{jm}^{(2)} \dot{W}_{1m} + \nu \sum_{m=1}^{N} C_{jm}^{(3)} W_{1m} \right) - \frac{2\pi R_{no1} C \beta}{A_{n1}} \left(W_{2j} - W_{1j} \right)
\end{aligned} \tag{B3}$$

$$\begin{aligned}
&\left(\frac{A_{n1} N_M}{A_{n2}} + \sum_{m=1}^{N} C_{jm}^{(1)} \Phi_{2m} - \Delta \right) \beta \sum_{m=1}^{N} C_{jm}^{(2)} W_{2m} + \beta \sum_{m=1}^{N} C_{jm}^{(1)} W_{2m} \sum_{m=1}^{N} C_{jm}^{(2)} \Phi_{2m} - \frac{I_{n2} \beta}{A_{n2}} \sum_{m=1}^{N} C_{jm}^{(4)} W_{2m} + \alpha^2 \beta \sum_{m=1}^{N} C_{jm}^{(2)} \ddot{W}_{2m} \\
&-\left(\frac{A_{n1} N_M}{A_{n2}} + \sum_{m=1}^{N} C_{jm}^{(1)} \Phi_{2m} - \Delta \right) \alpha^2 \beta \sum_{m=1}^{N} C_{jm}^{(4)} W_{2m} - \alpha^2 \beta \left(3 \sum_{m=1}^{N} C_{jm}^{(3)} W_{2m} \sum_{m=1}^{N} C_{jm}^{(2)} \Phi_{2m} + 3 \sum_{m=1}^{N} C_{jm}^{(2)} W_{2m} \sum_{m=1}^{N} C_{jm}^{(3)} \Phi_{2m} \right) \\
&-\alpha^2 \beta \left(\sum_{m=1}^{N} C_{jm}^{(1)} W_{2m} \sum_{m=1}^{N} C_{jm}^{(4)} \Phi_{2m} + \sum_{m=1}^{N} C_{jm}^{(1)} W_{2m} \sum_{m=1}^{N} C_{jm}^{(4)} \Phi_{2m} \right) + \left(\frac{I_{n2} \beta}{A_{n2}} \right) \sum_{m=1}^{N} C_{jm}^{(2)} \ddot{W}_{2m} - \beta \ddot{W}_{2j} \\
&+\frac{2\alpha^2 \beta \pi R_{no2}}{A_{n2}} \left(K_{nw} \sum_{m=1}^{N} C_{jm}^{(2)} W_{2m} - K_{nG} \sum_{m=1}^{N} C_{jm}^{(4)} W_{2m} \right) + \frac{2\alpha^2 \beta C \pi R_{no1}}{A_{n2}} \left(\sum_{m=1}^{N} C_{jm}^{(2)} W_{2m} - \sum_{m=1}^{N} C_{jm}^{(2)} W_{1m} \right) - \frac{I_{n2} \alpha^2 \beta}{A_{n2}} \sum_{m=1}^{N} C_{jm}^{(4)} \ddot{W}_{2m} = \\
&\frac{2\pi R_{no2} \beta}{A_{n2}} \left(K_{nw} W_{2j} - K_{nG} \sum_{m=1}^{N} C_{jm}^{(2)} W_{2m} \right) + \frac{2\pi C \beta R_{no1}}{A_{n2}} \left(W_{2j} - W_{1j} \right)
\end{aligned} \tag{B4}$$

© 2012 IAU, Arak Branch

www.SID.ir

Archive of SID

$$\sum_{m=1}^{N} C_{jm}^{(2)} \Phi_{1m} - H \sum_{m=1}^{N} C_{jm}^{(2)} U_{1m} - H\beta^2 \sum_{m=1}^{N} C_{jm}^{(1)} W_{1m} \sum_{m=1}^{N} C_{jm}^{(2)} W_{1m} = 0, \tag{B5}$$

$$\sum_{m=1}^{N} C_{jm}^{(2)} \Phi_{2m} - H \sum_{m=1}^{N} C_{jm}^{(2)} U_{2m} - H\beta^2 \sum_{m=1}^{N} C_{jm}^{(1)} W_{2m} \sum_{m=1}^{N} C_{jm}^{(2)} W_{2m} = 0. \tag{B6}$$

REFERENCES

[1] Xu X., 2010, Dynamic torsional buckling of cylindrical shells, *Computers and Structures* **88:** 322-330.

[2] Patel S.N., Datta P.K., Sheikh A.H., 2006, Buckling and dynamic instability analysis of stiffened shell panels, *Thin-Walled Structures* **44:** 321-333.

[3] Païdoussis M.P., 1998, Fluid–Structure Interactions: Slender Structures and Axial Flow, Academic Press, London.

[4] Amabili M., Pellicano F., Païdoussis M.P., 2002, Non-linear dynamics and stability of circular cylindrical shells conveying flowing fluid, *Computers and Structures* **80**: 899-906.

[5] Amabili M., Karagiozis K., Païdoussis M.P., 2009, Effect of geometric imperfections on non-linear stability of circular cylindrical shells conveying fluid, *International Journal of Non-Linear Mechanics* **44:** 276-289.

[6] Karagiozis K., Amabili M., Païdoussis M.P., 2010, Nonlinear dynamics of harmonically excited circular cylindrical shells containing fluid flow, *Journal of Sound and Vibration* **329**: 3813-3834.

[7] Païdoussis M.P., Chan S.P., Misra A.K., 1984, Dynamics and stability of coaxial cylindrical shells containing flowing fluid, *Journal of Sound and Vibration* **97**: 201-235.

[8] Ni Q., Zhang Z.L., Wang L., 2011, Application of the differential transformation method to vibration analysis of pipes conveying fluid, *Applied Mathimatics and Computation* **217:** 7028-7038.

[9] Yan Y., 2009, Dynamic behavior of triple-walled carbon nanotubes conveying fluid, *Journal of Sound and Vibration* **319**: 1003-1018.

[10] Yoon J., Ru C.Q., Mioduchowski A., 2005, Vibration and instability of carbon nanotubes conveying fluid, *Composite Science and Technology* **65:** 1326-1336.

[11] Wang L., 2009, Vibration and instability analysis of tubular nano- and micro-beams conveying fluid using nonlocal elastic theory, *Physica E* **41**: 1835-1840.

[12] Eringen A.C., 1983, On differential equations of nonlocal elasticity and solutions of screw dislocation and surface waves, *Applied Phyics* **54**: 4703–4710.

[13] Ke L.L., Wang Y.S., 2011, Flow-induced vibration and instability of embedded double-walled carbon nanotubes based on a modified couple stress theory, *Physica E* **43**: 1031-1039.

[14] Ghavanloo E., Daneshmand F., Rafiei M., 2010. Vibration and instability analysis of carbon nanotubes conveying fluid and resting on a linear viscoelastic Winkler foundation, *Physica E* **42:** 2218-2224.

[15] Khosravian N., Rafii-Tabar H., 2007. Computational modelling of the flow of viscous fluids in carbon nanotubes, *Journal of Physics D: Applied Phyics* **40:** 7046.

[16] Wang L., Ni Q., 2009, A reappraisal of the computational modelling of carbon nanotubes conveying viscous fluid, *Mechanics Resaserch Communication* **36**: 833-837.

[17] Salehi-Khojin A., Jalili N., 2008, Buckling of boron nitride nanotube reinforced piezoelectric polymeric composites subject to combined electro-thermo-mechanical loadings. *Composite Science and Technology* **68**: 1489-1501.

[18] Ghorbanpour Arani A., Amir S., Shajari A.R., Mozdianfard M.R., 2012, Electro-thermo-mechanical buckling of DWBNNTs embedded in bundle of CNTs using nonlocal piezoelasticity cylindrical shell theory, *Composite Part B: Engineering* **43:** 195-203.

[19] Mosallaie Barzoki A.A., Ghorbanpour Arani A., Kolahchi R., Mozdianfard M.R., 2012, Electro-thermo-mechanical torsional buckling of a piezoelectric polymeric cylindrical shell reinforced by DWBNNTs with an elastic core, *Applied Mathimatical Modelling* **36**: 2983-2995.

[20] Chen L.W., Lin C.Y., Wang C.C., 2002, Dynamic stability analysis and control of a composite beam with piezoelectric layers, *Composite Structures* **56**: 97-109.

[21] Mohammadimehr M., Saidi A.R., Ghorbanpour Arani A., Arefmanesh A., Han Q., 2010, Torsional buckling of a DWCNT embedded on winkler and pasternak foundations using nonlocal theory, *Journal of Mechanical Science and Technology* **24**: 1289-1299.

[22] Ghorbanpour Arani A., Mosallaie Barzoki A.A., Kolahchi R., Loghman A., 2011, Pasternak foundation effect on the axial and torsional waves propagation in embedded DWCNTs using nonlocal elasticity cylindrical shell theory, *Journal of Mechanical Science and Technology* **25**: 2385-239.

[23] Ru C.Q,., 2001, Axially compressed buckling of a doublewalled carbon nanotube embedded in an elastic medium, *Journal of Mechanical Phyics and Solids* **49**: 1265-1279.

© 2012IAU, Arak Branch

Archive of SID

www.SID.ir

[24] Ghorbanpour Arani A., Hashemian M., Loghman A., Mohammadimehr M., 2011, Study of dynamic stability of the double-walled carbon nanotube under axial loading embedded in an elastic medium by the energy method, *Journal of Applied Mechanic Technology and Phyics* 52: 815-824.
[25] Kuang Y.D., He X.Q., Chen C.Y., Li G.Q., 2009, Analysis of nonlinear vibrations of double-walled carbon nanotubes conveying fluid, *Computational Material Science* **45:** 875-880.
[26] Reddy J.N, 2007, Nonlocal theories for bending, buckling and vibration of beams, *International Journal of Engineering and Science* **45**: 288-307.
[27] Yang J., 2005, AN Introduction to the theory of piezoelectricity, Springer, USA.
[28] Ke L.L., Xiang Y. , Yang J., Kitipornchai S., 2009, Nonlinear free vibration of embedded double-walled carbon nanotubes based on nonlocal Timoshenko beam theory, *Computational Material Science* **47:** 409-417.
[29] Ansari R., Gholami R., Sahmani S., 2012, On the dynamic stability of embedded single-walled carbon nanotubes including thermal environment effects, *Scientia Iranica* **19**: 919–925.

Archive of SID

© 2012 IAU, Arak Branch

www.SID.ir